Aberrant modularity and lower resiliency of structural covariance network in first-episode antipsychotic-naive psychoses

Madison Lewis, BS[1]

Tales Santini, PhD[1]

Nicholas Theis, MS[2]

Brendan Muldoon, BS[2]

Matcheri S. Keshavan, MD[3]

Konasale M. Prasad, MD[1,2,4*]

[1]Department of Bioengineering, Swanson School of Engineering, University of Pittsburgh, PA 15213

[2]Department of Psychiatry, University of Pittsburgh School of Medicine, Pittsburgh, PA 15213

[3]Department of Psychiatry, Beth Israel Deaconess Medical Center, Harvard Medical School, Boston, MA

[4]Veterans Affairs Pittsburgh Health System, University Drive, Pittsburgh, PA 15240

*Corresponding author:
3811 O'Hara St
Pittsburgh, PA 15213
Email: Prasadkm@upmc.edu

Running Title: Structural covariance network in first-episode antipsychotic-naïve psychoses

The results of this manuscript were presented at the 74th Annual Meeting of the Society of Biological Psychiatry held on May 16 to 18, 2019 at Chicago, IL

Abstract

Objective: Structural brain alterations are consistently observed in schizophrenia. However, divergent findings suggest that often-observed regions exist within a network of susceptible regions. We conducted structural covariance analysis of multiple morphometric features of 358 regions from 79 first-episode anti-psychotic-naive psychosis patients (FEAP) and 68 healthy controls to investigate network differences.

Methods: Using graph theoretic methods, we investigated structural covariance network of Freesurfer-derived cortical gray matter volumes, thickness, curvature, and surface area using the Brain Connectivity Toolbox within MATLAB, compared network modularity using the Community Detection Toolbox within MATLAB, and examined the resilience of the network using simulated attacks.

Results: FEAP showed decreased heterogeneity of cortical volumes compared to controls which was driven by decreased heterogeneity of cortical thickness but not surface area. Reduced morphological heterogeneity was associated with less differentiated community structure in FEAP compared to controls. FEAP patients, in general, showed less resilient networks that were more vulnerable to attacks on fewer nodes compared to healthy subjects.

Conclusions: Our findings of decreased heterogeneity may be associated with FEAP-related pathology since the impact of illness chronicity and treatment are minimized. Contribution of cortical thickness but not surface area covariance network suggests that neurodevelopmental processes affecting the thickness rather than the surface area may be pathophysiologically more significant.

Key words: Network neuroscience; Computational psychiatry; Structural covariance network; Graph theory; Schizophrenia; Morphometry; Neuroimaging; Magnetic resonance imaging

Introduction

Schizophrenia is associated with widespread morphometric alterations in volume, cortical thickness, and surface area of the brain. Altered morphometry in approximately 50 different regions have been associated with schizophrenia although findings are inconsistent [1, 2]. Inconsistent findings may be due to heterogeneity of illness, stage of the illness and medication status. Inconsistencies may also be due to different brain regions within a network showing different degrees of covariations among other region such that cross-sectional examination allows identifying a few regions to be showing group differences. Such a possibility can be tested by examining structural covariance networks (SCN) of brain regions. SCNs are quantitative mathematical representation of covariation of regional morphometric measurements (volume, cortical thickness, and surface area). A possibility of such covariation is supported by between-subject variability of regional volumes being greater than between-subject differences in whole brain volume and between-subject differences in one region covarying with between-subject differences in other regions [3, 4]. Thus, SCNs can potentially highlight between-subject differences in regional morphometrics covarying with between-subject differences in other brain regions that cannot be tested by between-group comparisons of individual or sets of regions-of-interest (ROI). These covariance patterns have revealed regional structural 'connectivity' differences in schizophrenia compared to controls [5] globally as well as regionally in relation to specific cognitive networks [5, 6]. Although the SCNs do not reflect underlying white matter tracts, white matter tracts tend to correspond to the SCN edges [7].

Existing studies have used different atlases, e.g., the Desikan-Killiany-Tourville (DKT) [8] and the Automated Anatomical Labeling (AAL) [9, 10] atlases based on anatomical landmarks or cytoarchitectonic patterns that may or may not reflect structural or functional connectional patterns. We used the Human Connectome Project (HCP) Atlas which parcellates the cortex into 358 regions based on connectivity, that allows for better functional/connectional interpretations of the results. These regions were delineated based on cortical architecture, function, connectivity, and topography which provides better information about the structural connectivity between the parcellated regions. More refined parcellation can potentially provide better data on covariance structure of the regions. For example, Mitelman et al [11] examined covariance of whole thalamic volume with cortical Brodmann areas and did not find correlations in patients but when volumes of thalamic nuclei were examined, patients showed correlation of pulvinar with frontal cortical BAs and controls with centromedian nucleus [12].

To our knowledge, this is the first study to use the HCP atlas to examine SCN in schizophrenia using a graph theoretic approach. We calculated graph metrics of the SCNs for segregation (clustering coefficient and modularity), integration (characteristic path length and eccentricity), centrality (betweenness centrality), and resilience (assortativity). In addition to comparing these graph measures between the study groups, we identified network hubs (highly connected nodes) because these nodes are important to the functioning of the network and paths of several nodes traverse through the hubs. Since schizophrenia SCN has been reported to be less resilient compared to healthy counterparts [9], we examined the schizophrenia SCN's resilience compared to that of healthy controls (HC) using the SCN built on HCP parcellated regions. We used the identified hubs to investigate their importance to the network stability and association of network characteristics with clinical phenotypes.

We examined 79 FEAP to minimize the impact of medication use and illness chronicity compared to group-matched 68 HC subjects. Although there were 13 studies that investigated the SCN of SZ using graph theory [5, 8, 9, 13-19], 3 studies investigated the FEAP patients and reported higher degree nodes in patients and no difference between first episode and chronic patients [8]. Path length and global efficiency did not show differences over 6 weeks, but clustering coefficient, local efficiency and modularity were different at the baseline timepoint but not at 6 weeks [19]. First episode schizophrenia SCN, but not chronic or treatment resistant schizophrenia, showed significant covariance difference with HC in the subnetwork comprising of temporal and frontal regions [16].

We hypothesized that the FEAP network will show higher degree, more hubs, and be less resilient compared to HC network based on previous publications that showed higher degree nodes [8, 9], higher number of hubs [10] that were quantitatively different from that of healthy controls [13]. These studies did not examine FEAP and examining this sample could highlight SCN connectivity before exposure to antipsychotics. Prior data on reduced network resilience in chronic SZ patients [9] has not been tested in FEAP. This is important because previous studies have shown increasing structural covariance strength as the disease progresses. Since the disease-related pathology starts well before the clinical manifestations, identifiable in the neonatal infants of schizophrenia patients [20], we predict that the resilience of the SCN of FEAP patients will be less than that of healthy controls. An additional innovative aspect of our study is that we have examined a network using a more refined atlas built that uses a parcellation scheme based on functional connectivity data. This approach could provide a better understanding of dysconnectivity and the impact of pathology in the hubs.

Methods

Subject Recruitment

We recruited FEAP patients of both sexes between the ages 12 and 50 years diagnosed per DSM-IV from inpatient and outpatient facilities of the Western Psychiatric Institute and Clinic, Pittsburgh. We excluded individuals with mental retardation per DSM IV, substance dependence within the past 6 months and/or substance abuse in the last month, significant medical/neurological disorders and prior antipsychotic treatment [21]. Consensus diagnosis was made by senior clinicians after reviewing the Structured Clinical Interview for DSM IV (SCID-IV; First 1997) and medical records data, and follow-up of patients for about six months. The study was approved by the Institutional Review Board of the University of Pittsburgh. After complete description of the study, informed consent was obtained from all subjects.

Imaging Methods

Details of MRI scanning were published [21]. Briefly, T1-weighted 3-dimensional spoiled-gradient-recalled (3D-SPGR) MRI data were acquired on a 1.5T GE whole-body scanner. We obtained 124 contiguous coronal slices of 1.5-mm thickness perpendicular to the anterior commissure-posterior commissure (AC-PC) line in steady-state pulse sequence (TE=5 msec, TR=25 msec, matrix=256x192, FOV=24 cm and flip angle=40°).

Preprocessing

Using FSL 6.0, the images for both groups were corrected for motion and bias distortion, and then skull-stripped. The initial parcellation was performed using the DKT atlas [22] within the Freesurfer 6.0. The cortical regions were further parcellated using the HCP atlas [23], which consist of 180 cortical regions per hemisphere created based on a large sample of resting state and task-based functional connectivity data. The HCP parcellation was integrated into the Freesurfer parcellation using publicly available Freesurfer's fsaverage space[24]. The parcellations were then mapped into the individuals' T1-weighted image space and had the volume, surface area, cortical thickness, and volume masks extracted for the network analysis. The images and segmentations were then visually inspected for quality. We did not observe any scan failing for poor quality parcellation.

SCN Construction

Using the volume, surface area, and cortical thickness, separate SCNs were constructed using partial correlation coefficients controlling for age, sex, and total brain volume. Additionally, a random graph was constructed from the group data by randomizing each edge 100 times. Construction and analyses of the SCN consisting of a 358x358 matrix filled with edges that represent structural correlations between regions were done using MATLAB (v9.6).

Finding a Threshold Range

First, we examined the distribution of graph measures with a threshold sweep using intensity threshold that was computed by choosing a strength and eliminating any of the edges below that value. Intensities from 0 (includes all edges) to 1 (excludes all edges) were examined at intervals of 0.025. At each threshold value across the intensity range, modularity, characteristic pathlength, clustering coefficient, and betweenness centrality were calculated using the Brain Connectivity Toolbox [25]. These measures were chosen to evaluate community structure, efficiency, and centrality of the SCN. To further investigate these measures, a range of intensity threshold was found to ensure that the analyses were applied to a network that closely resembled a biological network. This range was calculated based on the small worldness of the network at each threshold value to ensure that these networks were nonrandom. Small worldness (σ) is calculated by comparing the clustering coefficient and the pathlength of the SCN with the random SCN:

$$\sigma = \frac{C/C_R}{L/L_R} \qquad (1)$$

where C is the clustering coefficient and L is the pathlength [13]. The minimum threshold value was chosen when all SCNs constructed for each threshold differed from a random graph (σ >1.2) and the maximum threshold value was chosen when the graphs above that threshold were no longer fully connected. A reachability matrix was calculated to determine whether the networks were fully connected using the brain connectivity toolbox.

Calculating Graph Measures

At threshold intervals of 0.025 across the small worldness range, we calculated importance degree), integration (characteristic path length and eccentricity), segregation (clustering coefficient and modularity), centrality (betweenness centrality), and resilience (assortativity) measures for the SCNs for

each group for each of the three morphometric measures [25]. Modularity, characteristic pathlength and assortativity were calculated at the global level and other metrics at the nodal level. The measures at the nodal level were then averaged and the group-level differences were tested using t-tests.

Identifying the Network Hubs

For further investigation into the network characteristics, the hubs were identified for each group. A region was defined as a hub if the regional degree, betweenness centrality, or eigenvector centrality were 2 standard deviations greater than the network average for these measures [13]. The hubs were calculated over the small worldness range at intervals of 0.005 to oversample the nodal measures. To identify critically important nodes as hubs, we conservatively selected the hubs that were found in ≥90% of the thresholded networks. Prior studies have defined hubs when they were found in 50% of the thresholded networks.

Examination of Network Resilience

We, next, examined the modularity of the network to investigate the network organization. We examined the subdivisions of the network (modules) at 21 different thresholds across the small worldness range as we did to identify the hubs. Circular graphs using NeuroMarvl (https://immersive.erc.monash.edu/neuromarvl/) show modules at 0.225 threshold. Next, we simulated "attacks" on the network by sequentially "removing nodes" without replacement for volume, cortical thickness, and surface area. All simulations were done using the volume SCN. The simulations using cortical thickness and surface area SCNs can be found in supplemental materials. The simulations were implemented across the entire small worldness-based threshold range at 0.025 intervals.

Simulation 1: We calculated the giant connected component (GCC) and average global efficiency of the network following "attack" (removal) of the hubs based on the descending order of betweenness centrality until all hubs were removed. Separately, we removed the hubs based on eigenvector centrality. We did not remove the hubs based on degree because all hubs based on degree were also identified based on one of the other two measures.

Simulation 2: Nodes were removed sequentially in a descending order of degree, betweenness centrality and eigenvector centrality separately until no more nodes were in the network. These measures were selected because the hubs were calculated based on these measures, and removing the hubs should affect the network more than removing other nodes. GCC and average efficiency of the network were measured.

Simulation 3: We ordered the nodes sequentially based on the graph measures that were significantly different between groups (average degree, clustering coefficient, and betweenness centrality and assortativity). We sequentially removed the nodes in 20th, 40th, 60th, and 80th percentile of the degree with replacement of all nodes back into the network at the beginning of a new percentile group.

Statistical Methods

T-tests were used to evaluate group differences in age before and after quality control, for global graph measures across the thresholds within the small world range, and for nodal graph measures. Chi squared test was used to compare sex distribution between the groups. Between-group morphometric comparison was performed using MANCOVA by including age, sex, and total brain volume as covariates.

Results

Clinical and Demographic

The final sample, after quality control, that consisted of 79 FEAP patients (mean age=23.99±7.21 years; 56 males) and 68 controls (mean age=24.59±6.64 years; 39 males) did not differ in age (t=0.52, df=145, p=0.60) and sex (χ^2=2.93, df=1, p=0.09). Mean illness duration from the time of first psychotic symptom to MRI was 2.57±3.35 years. There was no significant difference between the age and sex of subjects whose scans were excluded because of poor segmentation compared to subjects whose scan data was included (FEAP=9, age=25.60±4.72 years; HC=8, age=21.83±5.20 years; t=1.57, df=15, p=0.14).

Morphometric Comparisons

Seventy-three regional measurements were different between groups across all three morphometrics. Two regions were significantly different using all three morphometrics: Left Area PGs and Right Area TE1 Middle. All group differences were of small effect sizes (Table 1).

Threshold Sweep and Graph Measures

Threshold sweep for characteristic pathlength, betweenness centrality, clustering coefficient and modularity for volume, thickness, and surface area showed group differences using intensity threshold for all three morphometric measures. The small worldness (σ) range for the SCNs in our study was between 0.175 and 0.275. We calculated the graph metrics at five thresholds across this threshold range. Figure 2 shows the global and figure 3 shows the nodal measures.

In the volume SCN, characteristic pathlength, modularity and assortativity were significantly higher among patients compared to controls (p<0.05) whereas characteristic pathlength and modularity were lower in the thickness SCN (Fig 2). For the volume SCN, patients had lower degree and higher clustering coefficient, betweenness centrality, and eccentricity compared to controls. In the cortical thickness SCN, patients had higher degree, clustering coefficient, and eccentricity. No difference between groups when using surface area SCN (Fig 3) (Table 2).

Table 2: Global and nodal graph metric differences between FEAP and Controls

Graph Measure	Volume SCN	Cortical Thickness SCN	Surface Area SCN
Global SCN metric			
Characteristic Pathlength	↑	↓	↔
Modularity	↑	↓	↓
Assortativity	↑	Dependent on Threshold	Dependent on Threshold
Nodal SCN Metric			
Degree	↓	↑	↔
Clustering Coefficient	↑	↑	↔
Betweenness Centrality	↑	↔	↔
Eccentricity	↑	↑	Dependent on Threshold

Hubs in FEAP and Controls

Numerically higher number of hubs were found in the volume and surface area SCN of FEAP, but the same number of hubs were found between the groups for the cortical thickness SCN (Table 3). Each hub in patients was unique with no shared hubs with HCs in the volume or cortical thickness networks. Two hubs were shared between the groups in the surface area networks. SZ hubs tend to be located in insular, opercular, and auditory areas. The HC hubs were mostly located in visual, parietal, and insular areas. Although some of the hub regions

for the SZ group are involved in high level functioning tasks, the SZ hubs lack the multimodal integration areas that were in the HC hubs. The module organization of the hubs can be viewed in figures 4 and 5.

Table 3: Hubs in FEAP and controls in the volume, surface area and cortical thickness SCNs

Volume SCN		Surface area SCN		Thickness SCN	
FEAP	**Healthy Control**	**FEAP**	**Healthy Control**	**FEAP**	**Healthy Control**
L Ventral Area 6	L Fourth Visual Area	L Area 47m	L Primary Motor Cortex	R Ventral Area 6	L Second Visual Area
L Posterior Insular Area 2	L Area V3A	L Area 47s	L Parieto-Occipital Sulcus Area 1	L Supplementary and Cingulate Eye Field	L Third Visual Area
L Frontal Opercular Area 4	L Parieto-Occipital Sulcus Area 2	L Area TA2	L Area OP4/PV	L Area PGs	L Fourth Visual Area
L Anterior Ventral Insular Area	L Intraparietal Sulcus Area 1	L Middle Insular Area	L Parabelt Complex	R Area 8BM	L Area IFSa
L Frontal Opercular Area 3	L V3B	L Frontal Opercular Area 3	R Area 10v	R Area 8B Lateral	L Inferior 6-8 Transitional Area
L Parabelt Complex	L Lateral Occipital 2	L Area STGa	R Frontal Opercular Area 3	R Area PFm Complex	L Area TE1 anterior
L Posterior Insular Area 1	L Temporoparieto-occipital Jn 3	L Auditory 5 Complex	R Parabelt Complex	L Area 47 lateral	R Third Visual Area
L Area Frontal Opercular 5	L Area PGp	L Area STSd anterior	R Lateral Belt Complex	R Area TG dorsal	R Area 6 anterior
R Primary Auditory Cortex	L Area Intraparietal 0	L Area TF	R Auditory 4 Complex	R Area PGp	L Area STSd anterior
R Posterior Insular Area 2	R Fourth Visual Area	L Area PH	L Frontal Opercular Area 3		
R Frontal Opercular Area 4	R Area V3A	L Area s32	R Primary Motor Cortex		
R Middle Insular Area	R Ventral Intraparietal Complex	L Auditory 4 Complex			
R Anterior Ventral Insular Area	R Dorsal Transitional Visual Area	R Frontal Opercular Area 4			
R Frontal Opercular Area 3	L Third Visual Area	R Area STGa			
R Parabelt Complex	L Dorsal Transitional Visual Area	R Area PF Opercular			
R Auditory 5 Complex	R Area 52	L Fusiform Face Complex			
R Area Frontal Opercular 5		L Area TE1 posterior			
L Medial Belt Complex		L Area PHT			
R Parieto-occipital Sulcus Area 1		R Frontal Opercular Area 3			
R Posterior OFC Complex					

Modular structure

There were seven modules among the FEAP and five in controls across 21 thresholds tested (Fig 4). The modules were qualitatively different between SZ and HC in that there was minimal overlap in the ROIs included in each module between the groups. For example, FEAP modules primarily consisted of auditory, limbic, and prefrontal nodes whereas modules of HC comprised of visual areas (See

Supplemental Table 1 and 2 for the regions in each module). Hubs were distributed across 4 communities in FEAP but in controls most of the hubs were in one community with one isolated hub in one community.

Network Resilience

Overall, each simulation showed the SZ SCN is less resilient to attack than the HC.

Simulation 1: We observed that both FEAP and HC showed the GCC size decreased for both groups with betweenness centrality-based or eigenvector centrality-based hubs were attacked with no group differences. The higher thresholded networks had lower efficiency and a more negative slope than the networks at a lower threshold (Fig 5).

Simulation 2: With sequential removal of nodes based on betweenness centrality and eigenvector centrality, betweenness centrality-based attacks showed group differences in GCC (Fig 6; see supplemental material eigenvector centrality-based attacks). The efficiency was not different between groups at any of the thresholds tested. There was no significant difference between the four thresholds tested when measuring GCC size. At 0.275, the GCC size breaks down and the network degrades for the SZ group at ~48.6% nodes removed and HC group at ~64.5% of nodes removed. Both simulation results show that thresholding has a significant impact on the network and its function.

Simulation 3: With percentile-based removal of nodes, the GCC decreased within each percentile group with no group differences. However, the global efficiency decreased more with the removal of nodes in FEAP although both controls and FEAP followed the same pattern.

Table 1: Morphometric differences in volume, cortical thickness and surface area between FEAP and controls of the regions that showed differences in at least two of the morphometric measure (The entire list is given in supplemental information).

Morphometric Comparisons- Multi-measure																		
	Cortical Thickness						Volume						Surface Area					
Region Name	FB Mean ± SD	HC Mean ± SD	Difference	ES	F	Sig.	FB Mean ± SD	HC Mean ± SD	Difference	ES	F	Sig.	FB Mean ± SD	HC Mean ± SD	Difference	ES	F	Sig.
Cortical Thickness, Volume, and Surface Area																		
L Area PGs	2.62±0.21	2.68±0.17	-2.28%	-0.33	4.57	0.03	2951.58±522.20	3215.93±535.80	-8.22%	-0.50	14.59	<.001	943.13±160.81	994.78±154.31	-5.19%	-0.33	6.70	0.01
R Area TE1 Mid	2.61±0.32	2.71±0.26	-3.63%	-0.34	4.59	0.03	1507.3±386.79	1669.68±345.16	-9.72%	-0.44	12.94	<.001	475.16±89.13	498.01±80.94	-4.59%	-0.27	6.05	0.02
Volume and Surface Area																		
L Sup 6-8 Trans A							801.62±232.34	881.13±225.54	-9.02%	-0.35	7.99	0.01	242.49±51.40	252.46±41.75	-3.95%	-0.21	4.10	0.05
R A TE1 post							2910.16±594.02	3085.38±562.04	-5.68%	-0.30	8.30	0.01	875.67±159.26	911.49±144.90	-3.93%	-0.24	4.23	0.04
R Sixth Visual A							672.89±165.24	740.63±178.44	-9.14%	-0.39	7.99	0.01	365.76±74.25	385.87±74.25	-5.21%	-0.27	4.05	0.05
Cortical Thickness and Volume																		
L A 3a	1.87±0.11	1.91±0.10	-1.77%	-0.32	6.45	0.01	1147.54±133.58	1189.24±125.36	-3.51%	-0.32	6.05	0.02						
L A 47m	2.64±0.32	2.73±0.35	-3.40%	-0.28	4.11	0.04	409.22±102.11	427.59±86.22	-4.30%	-0.19	4.29	0.04						
L Ventral A 6	3.07±0.29	3.17±0.30	-2.96%	-0.32	4.64	0.03	991.78±216.26	1031.9±208.30	-3.89%	-0.19	3.98	0.05						
L A Ant 32 prime	2.74±0.19	2.84±0.19	-3.44%	-0.52	13.75	<.001	895.63±256.05	976.47±237.16	-8.28%	-0.33	7.36	0.01						
L Inf 6-8 Trans A	2.61±0.22	2.71±0.24	-3.67%	-0.44	9.08	0.01	1078.41±252.64	1162.15±321.97	-7.21%	-0.29	5.26	0.02						
L A TE1 post	2.68±0.22	2.75±0.21	-2.54%	-0.33	5.82	0.01	3427.46±618.30	3575.09±570.00	-4.13%	-0.25	6.14	0.01						
R A OP2-3/VS	2.72±0.23	2.79±0.25	-2.34%	-0.27	4.17	0.04	428.49±58.04	443.29±77.15	-3.33%	-0.22	4.60	0.03						
R Suppl & Cing Eye Field	2.93±0.29	3.05±0.23	-3.70%	-0.44	8.80	0.01	1533.77±274.76	1587.84±260.28	-3.41%	-0.20	5.45	0.02						

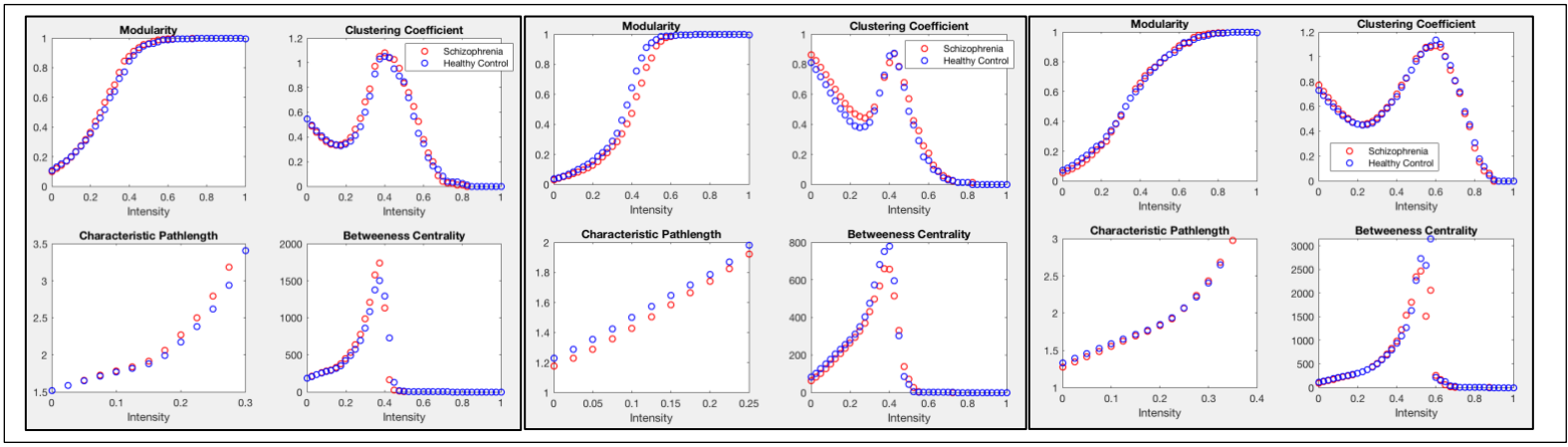

Figure 1: Threshold sweep using an intensity threshold for the volume (left), cortical thickness (middle) and surface area (right) SCNs.

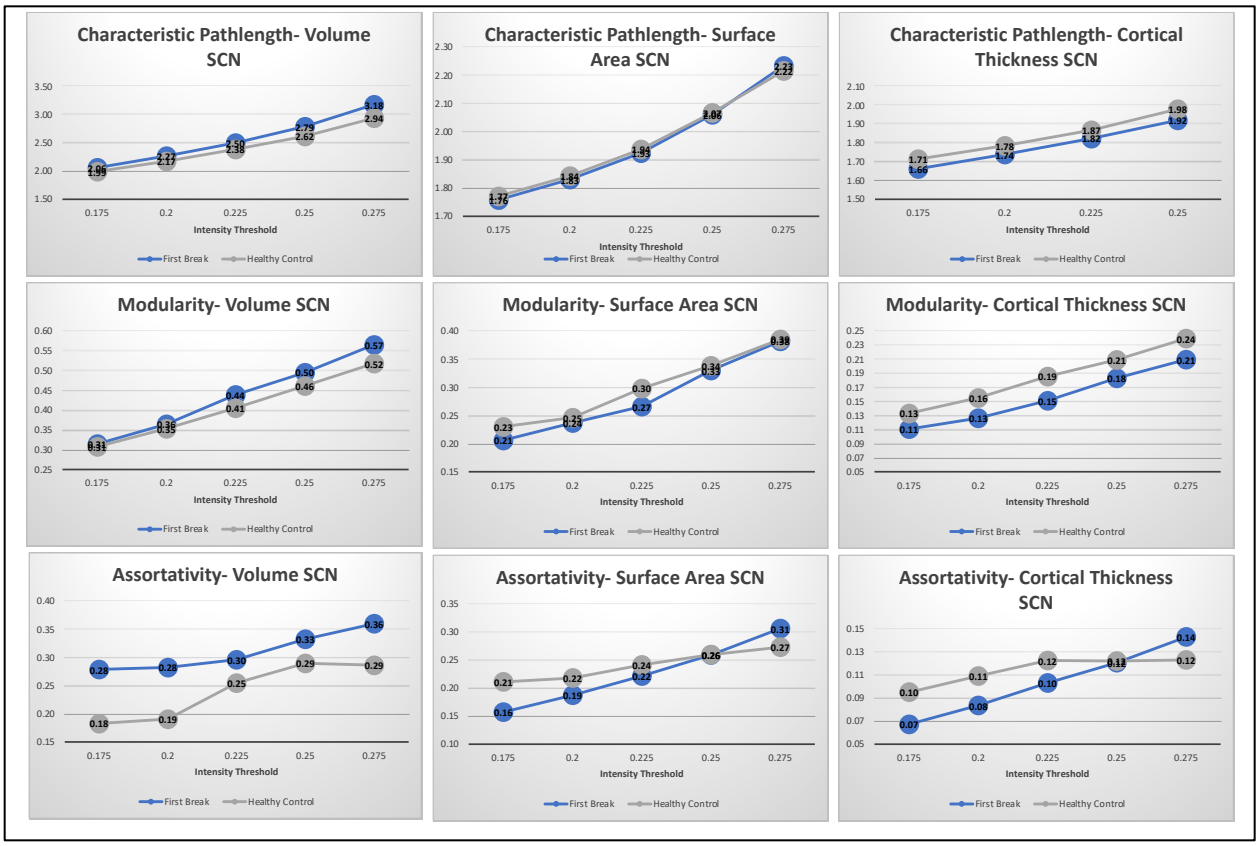

Figure 2: Gobal graph measures between first break (blue) and healthy control (gray) across five thresholds in our small-worldness range.

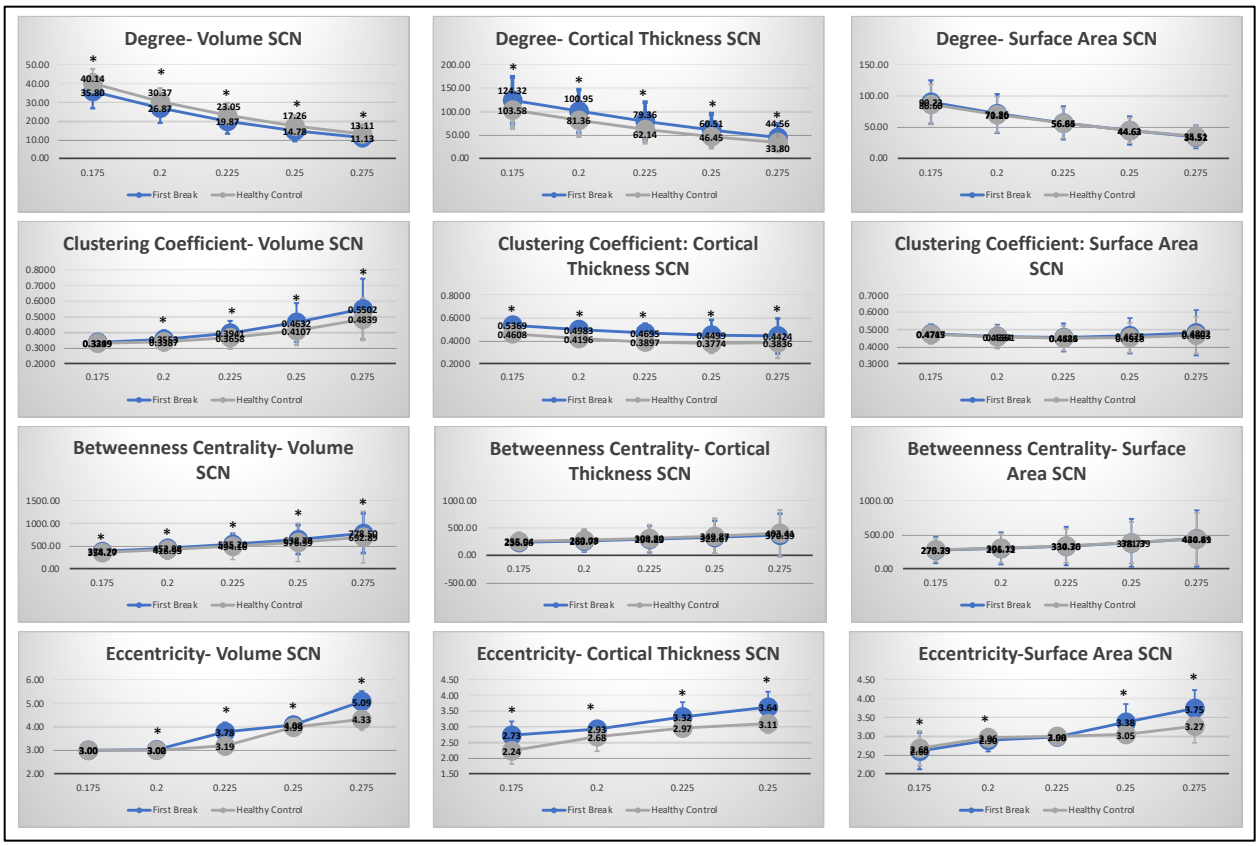

Figure 3: Average nodal graph measures between first break and healthy control across five thresholds in our small-worldness range. * represents significant difference between groups ($p<0.05$).

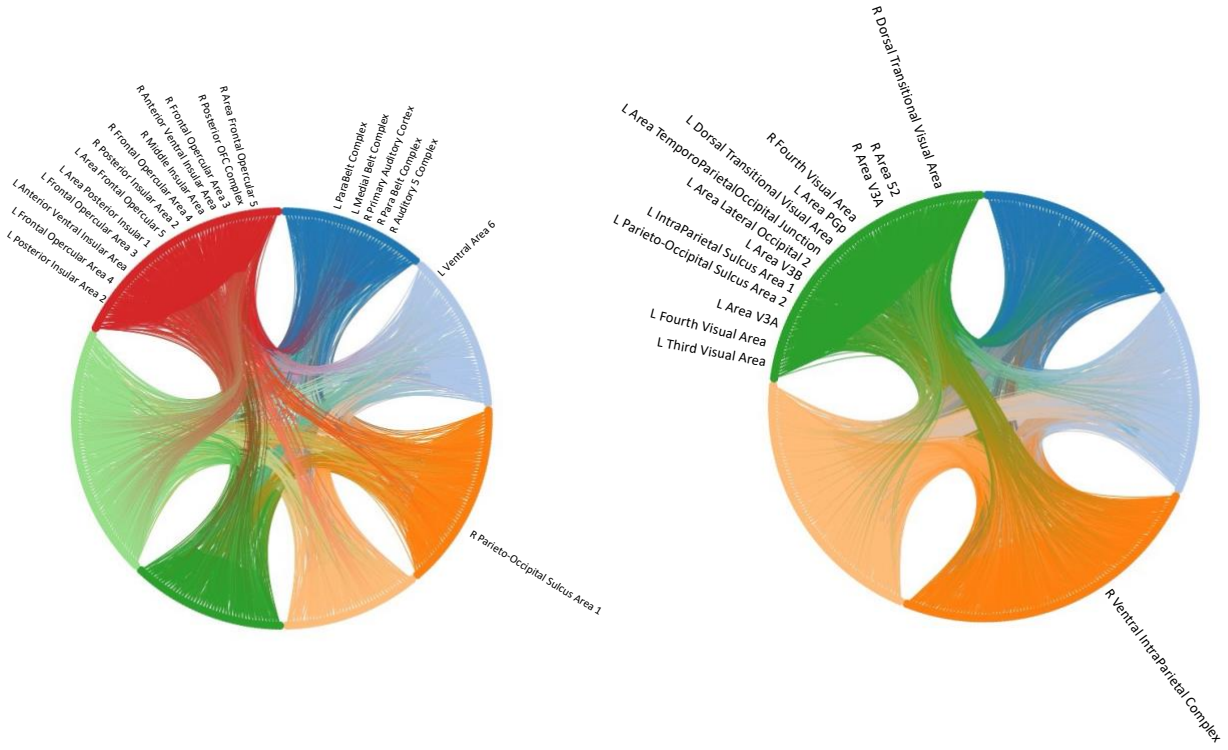

Figure 4: First Break (Left) and healthy control (right) circular network diagram organized by module number with hubs labeled.

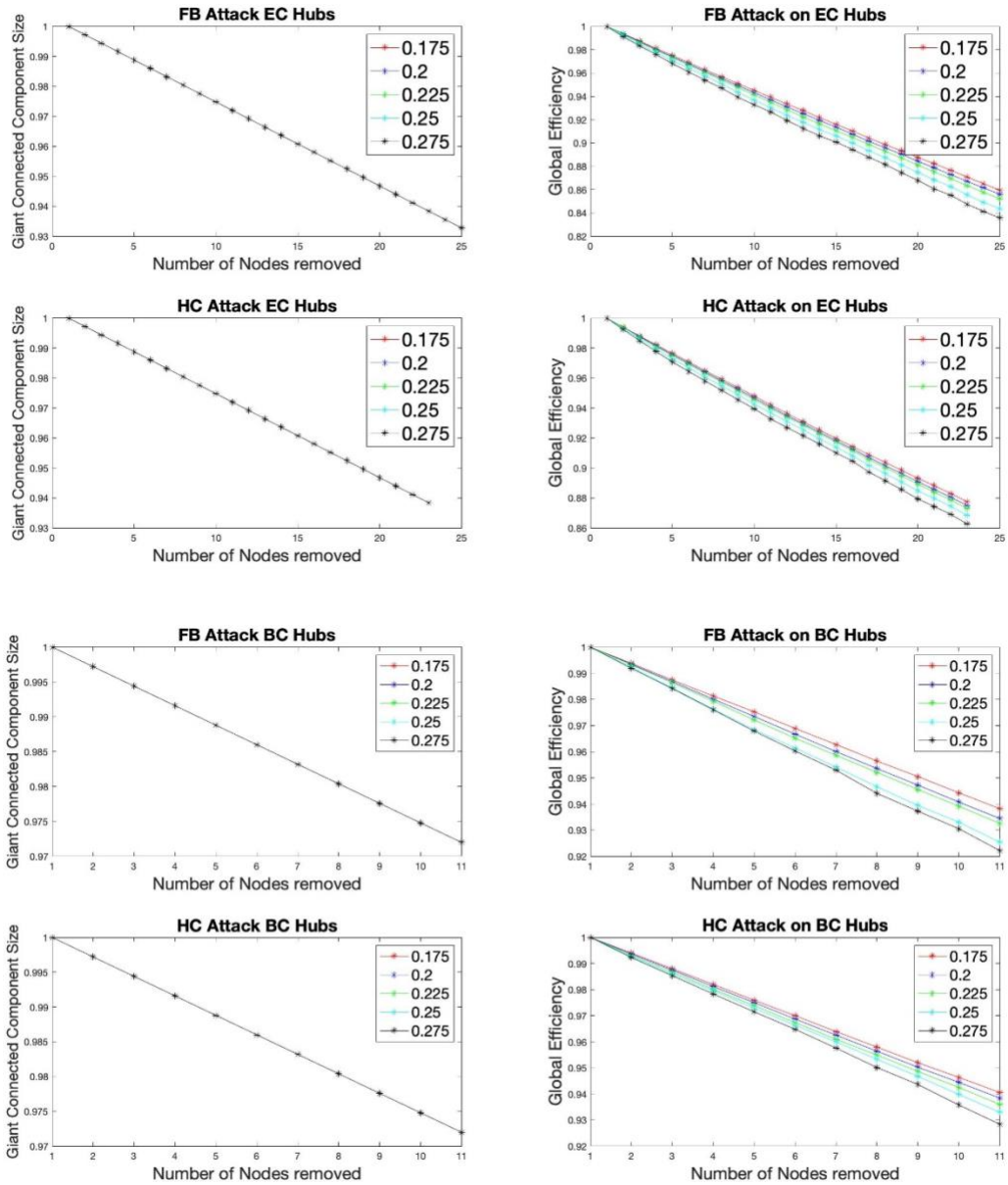

Figure 5: Giant connected component size and efficiency of the network after each node removal based on hubs. SZ on the top and HC on the bottom. (Volume SCN, other morphometric SCNs are in supplementary information)

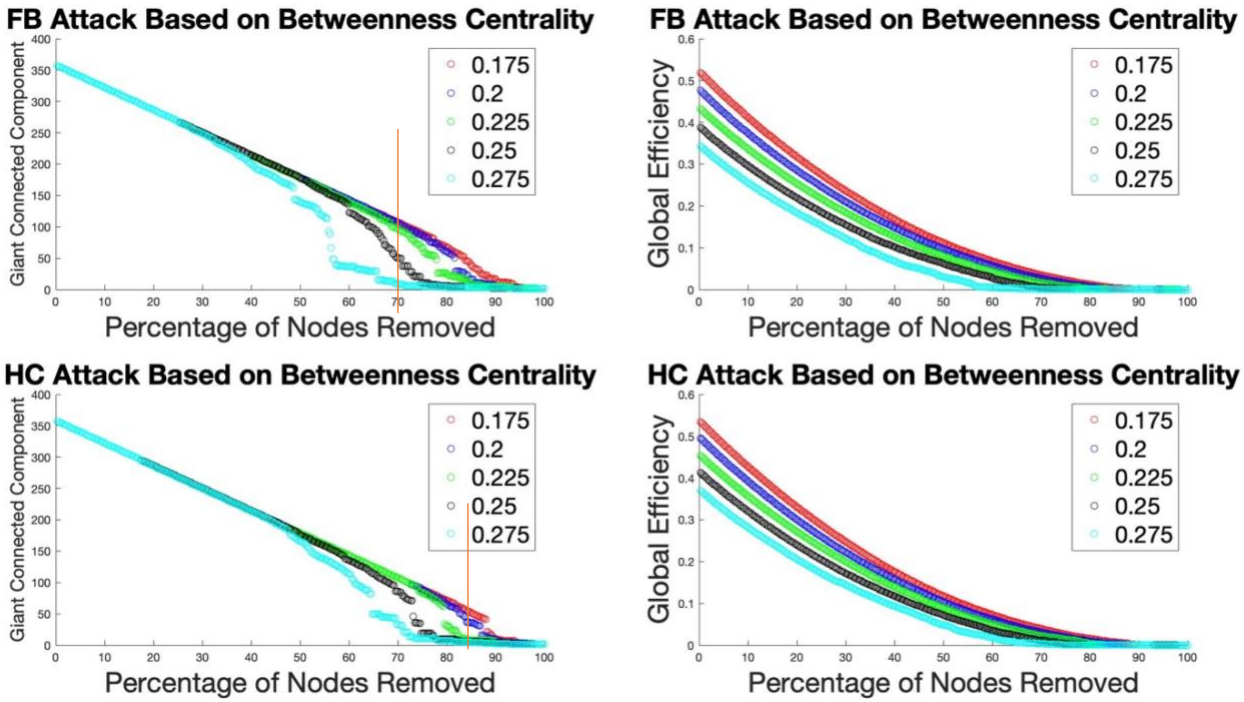

Figure 6: Giant connected component size and efficiency of the network after each node removal based on betweenness centrality using volume SCNs. FB on the top and HC on the bottom at different thresholds across small worldness range.

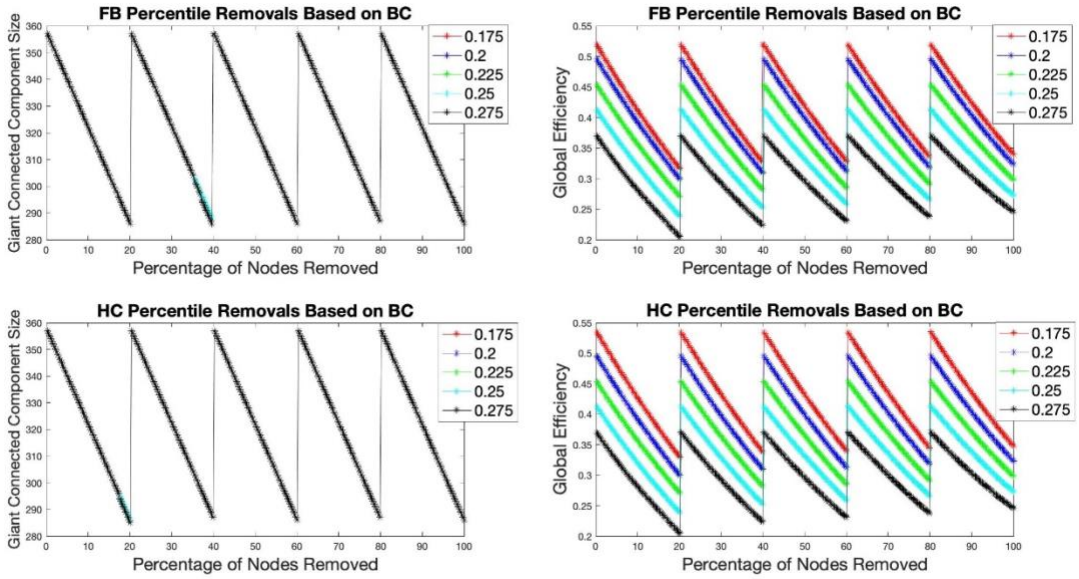

Figure 7: Removals based on graph measure percentiles (Top 20, 40, 60, 80, 100) with replacement at the beginning of each percentile. (Volume SCN, other morphometric SCNs are in supplementary information)

Discussion

Our study is the first to use fine grained, functional connectivity-based HCP parcellation to examine covariation of brain regions in first-episode antipsychotic-naïve patients with psychoses compared to healthy controls, to the best of our knowledge. In addition, we have examined all three major morphometric components (volume, cortical thickness, and surface area) to elucidate differential contribution of thickness and surface area to the volume SCN. The main findings of our study are that the FEAP subjects showed higher characteristic pathlength, modularity and assortativity compared to controls whereas cortical thickness showed lower values among the global graph measures. Among the nodal measures, clustering coefficient, betweenness centrality and eccentricity were higher in the volume SCN and showed a general trend in the same direction in the thickness SCN among FEAP compared to controls. There were higher number of hubs and modules in patients compared to controls; however, the hubs and modules were comprised of distinctly different nodes between the two groups. In addition, the FEAP network was less resilient to "attacks" than the healthy control network. These findings suggest that the FEAP SCN consists of longer pathlengths, greater tendency to form communities, higher likelihood of similar nodes connecting with each other, higher frequency of connecting with neighboring nodes, and the greater importance of nodes in the shortest paths compared to controls. Further, the communities were formed by regions from across different lobes of the brain in FHR than being more organized as in controls. Hubs were distributed across more communities in patients than in controls. Thus, qualitatively different SCN in FEAP may underlie some of the disease-related clinical manifestations.

Investigation of cortical thickness and surface area-derived SCNs show that the main contributions may have been from the cortical thickness rather than by the surface area since volume=surface area*thickness. Characteristic path length, which is a typical separation between two nodes – a global network property - was higher in FEAP suggesting more "intermediary states" among nodes and higher small worldness of FEAP SCN. Longer path length also suggests that the FEAP networks are shifted away from randomized configuration compared to HC SCN [26] and less closer interaction between the nodes. This network state could introduce greater chances of network breakdown in the network that may not allow for more adaptive nodal interactions. A recent analysis showed that significantly shorter pathlength allowed greater chances of close physical interaction among proteins in protein-protein interaction network in schizophrenia [27]. Thus, longer path lengths as seen in FEAP SCN may prevent such interactions that may be required for more normal communication among the nodes. Functional connectivity networks have also shown longer pathlength in schizophrenia [28]. Thus, investigation of multiple layers of networks simultaneously can provide greater insight into the network properties and functional implications.

The cortical thickness but not surface area SCN of FEAP was also significantly different from HC SCN. Since volume is a product of surface area and thickness, our findings suggest that the disease/developmental processes may preferentially affect thickness rather than surface area. Cortical thickness is related to laminar architecture and is highly conserved phylogenetically [29]. Existing data shows that the cortical thickness increases from early gestation period until early postnatal life [30], increases by about 36% from birth to age 2 years when it nearly reaches its adult value, after which, it starts decreasing from 5 years of age in the sensorimotor areas first, followed by frontal lobe and then, the posterior parietal cortex until

approximately 20 years of age [31]. Cortical thickness changes are governed by cellular processes such as alterations in neuropil density, neuronal packing density, soma volumes, and myelination.[32] For these reasons, association of cortical thickness network properties may be related to altered neurodevelopment. This is supported by observations of differential growth of inner and outer cortical layers [33-36], cortical development during the evolution [37], and animal studies [38]. Growth in surface area is closely tied to cortical curvature but driven by different processes. Cortical surface area continues to grow during childhood, achieving nearly 70% of its adult value by age 2 [30]. Some region-specific cortical thinning has been observed in schizophrenia [39, 40] and in familial high risk subjects who converted to psychosis [41, 42]. Thus, it is likely that the SCNs of gray matter volume represent changes in cortical thickness but less of surface area changes during childhood and adolescence. Although there is no direct evidence, it is possible that disease process of psychosis may impact neurodevelopment during the developmental windows when cortical thickness is actively going through changes.

Low average degree in volume SCN means that the number of edges connected to each node in the SZ SCN was lower than the number of edges on each node of the HC SCN. Since this is an average of all nodal degree measurements, it is possible to have a few nodes with high degree with a majority of nodes in the network having low degree. This is supported by finding more communities and hubs in FEAP SCN compared to HC SCN. Higher average clustering co-efficient and betweenness centrality further supports the presence of several high degree nodes in the FEAP network than in HC SCN.

Many outcomes of the graph measures were dependent on the threshold chosen showing that the graph is significantly altered depending on the threshold method. Small worldness-based threshold range provides a useful range to examine the network but does not provide one optimal threshold. This could be an issue when networks based on other modalities are tested together. We, recently, proposed a method that gives an optimal threshold and can be applied to networks built using imaging data across different modalities (BioArx).

Our finding of larger number of hubs in the SZ SCN is not consistent with previous finding [9]. This inconsistency may arise from the use of an atlas that parcellates brain into larger and comparatively fewer ROIs. Since the FEAP SCN is relatively sparsely connected, the FEAP SCN may rely on more hubs to keep the network “functional”. In addition, larger number of hubs could indicate that the network may not be efficient and needs more edges or nodes to connect from one region to another. Further, many of these hubs have been shown to be morphometrically abnormal in prior studies. Notably, none of the hubs in the FEAP SCN was in the heteromodal association area whereas many of HC SCN were in this region possibly suggesting that the FEAP SCN may be associated with large scale integration of multimodal information.

Because the FEAP network is sparsely connected with more hubs, we predicted the network to be less resilient than the HC when hubs were “attacked”. Our observation did not support our prediction. This differing result could be because of the difference in atlas choice. When one node is removed in the network in built on AAL-90 atlas [9], it is approximately equivalent to the removal of about 4 regions using the HCP atlas. Therefore, more nodes would have to be removed in our study to make a significant impact on our network. After removing the hubs, we decided to remove in sequential order of regions with high to low graph theory measurements to find which hubs may hold the network together. Attacking

betweenness centrality had the largest effect on the networks which suggests that hubs based on betweenness centrality, or nodes with high betweenness centrality, may be vital to keep the network functional. When comparing the effect on SZ vs HC networks, the SZ networks had no significant difference in the rate of change of the efficiency curve. The greatest connected component size curve did degrade quicker in the SZ network (~175 nodes removed) than the HC (~230 nodes removed). Since the efficiency of the network showed no significant difference between groups, this implies that the SZ network is more resilient to attack because although the network is breaking into smaller parts it is still able to have similar efficiency to the healthy control that has not broken up yet.

There are several strengths in our study. We have examined first-episode antipsychotic-naïve psychoses patients that minimizes the impact of duration of illness and medication use providing a better estimate of neurobiological correlates. Multiple morphometric measures simultaneously to comprehensively understand the SCN and its associations with the overall severity and functional status. We have applied appropriate multiple test corrections throughout the analyses where applicable and examined the data for possible outliers and used alternative statistical methods to ensure robustness of our observations. Limitations of our study includes modest sample size. Although imaging data were obtained on 1.5T scanner, the resolution was adequate to reliably measure the morphometric measures. This group-level structural covariance analysis may be sensitive to outliers. To address this, we kept the number of outliers low and covaried for age, sex and total brain volume using partial correlation. In addition, precise neurobiological impact of greater significance is difficult to quantify in macroscale networks averaged across the groups. Emerging methods, such as structural similarity network (SSN) [42] and individualized differential SCN [43] analyses produce morphological networks for each subject. It may be difficult to examine SSNs for each morphological feature by structural similarity. More work needs to be done to relate structural similarity analysis to structural covariance analysis to connect the clinical utility of the SSN with potential biological meaning of the SCN.

References

1. Shenton, M.E., et al., *A review of MRI findings in schizophrenia.* Schizophr Res, 2001. **49**: p. 1-52.
2. Wright, I.C., et al., *Meta-analysis of regional brain volumes in schizophrenia.* Am J Psychiatry, 2000. **157**(1): p. 16-25.
3. Lerch, J.P., et al., *Mapping anatomical correlations across cerebral cortex (MACACC) using cortical thickness from MRI.* Neuroimage, 2006. **31**(3): p. 993-1003.
4. Kennedy, D.N., et al., *Gyri of the human neocortex: an MRI-based analysis of volume and variance.* Cereb Cortex, 1998. **8**(4): p. 372-84.
5. Griffa, A., et al., *Characterizing the connectome in schizophrenia with diffusion spectrum imaging.* Hum Brain Mapp, 2015. **36**(1): p. 354-66.
6. Cauda, F., et al., *The morphometric co-atrophy networking of schizophrenia, autistic and obsessive spectrum disorders.* Hum Brain Mapp, 2018. **39**(5): p. 1898-1928.
7. Xu, L., G. Pearlson, and V.D. Calhoun, *Joint source based morphometry identifies linked gray and white matter group differences.* Neuroimage, 2009. **44**(3): p. 777-89.
8. Zugman, A., et al., *Structural covariance in schizophrenia and first-episode psychosis: An approach based on graph analysis.* J Psychiatr Res, 2015. **71**: p. 89-96.
9. Palaniyappan, L., et al., *Structural covariance and cortical reorganisation in schizophrenia: a MRI-based morphometric study.* Psychol Med, 2019. **49**(3): p. 412-420.
10. Zhang, Y., et al., *Abnormal topological organization of structural brain networks in schizophrenia.* Schizophr Res, 2012. **141**(2-3): p. 109-18.
11. Mitelman, S.A., et al., *Cortical intercorrelations of temporal area volumes in schizophrenia.* Schizophr Res, 2005. **76**(2-3): p. 207-29.
12. Mitelman, S.A., et al., *Correlations between volumes of the pulvinar, centromedian, and mediodorsal nuclei and cortical Brodmann's areas in schizophrenia.* Neurosci Lett, 2006. **392**(1-2): p. 16-21.
13. Bassett, D., et al., *Hierarchical Organization of Human Cortical Networks in Health and Schizophrenia*. 2008, Journal of Neuroscience.
14. Kuo, C.Y., et al., *Large-Scale Structural Covariance Networks Predict Age in Middle-to-Late Adulthood: A Novel Brain Aging Biomarker.* Cereb Cortex, 2020. **30**(11): p. 5844-5862.
15. Kim, S., et al., *Altered Cortical Thickness-Based Individualized Structural Covariance Networks in Patients with Schizophrenia and Bipolar Disorder.* J Clin Med, 2020. **9**(6).
16. Wannan, C.M.J., et al., *Evidence for Network-Based Cortical Thickness Reductions in Schizophrenia.* Am J Psychiatry, 2019. **176**(7): p. 552-563.
17. Palaniyappan, L., et al., *Abnormalities in structural covariance of cortical gyrification in schizophrenia.* Brain Struct Funct, 2015. **220**(4): p. 2059-71.
18. Liu, F., et al., *Altered voxel-wise gray matter structural brain networks in schizophrenia: Association with brain genetic expression pattern.* Brain Imaging Behav, 2019. **13**(2): p. 493-502.
19. Nelson, E.A., et al., *Gyrification Connectomes in Unmedicated Patients With Schizophrenia and Following a Short Course of Antipsychotic Drug Treatment.* Front Psychiatry, 2018. **9**: p. 699.
20. Shi, F., et al., *Altered structural connectivity in neonates at genetic risk for schizophrenia: a combined study using morphological and white matter networks.* Neuroimage, 2012. **62**(3): p. 1622-33.
21. Prasad, K.M., et al., *The entorhinal cortex in first-episode psychotic disorders: a structural magnetic resonance imaging study.* Am J Psychiatry, 2004. **161**(9): p. 1612-9.

22. Klein, A. and J. Tourville, *101 labeled brain images and a consistent human cortical labeling protocol.* Front Neurosci, 2012. **6**: p. 171.
23. Glasser, M.F., et al., *A multi-modal parcellation of human cerebral cortex.* Nature, 2016. **536**(7615): p. 171-178.
24. Mills, K., *HCP-MMP1.0 projected on fsaverage*, figshare, Editor. 2016.
25. Rubinov, M. and O. Sporns, *Complex network measures of brain connectivity: uses and interpretations.* Neuroimage, 2010. **52**(3): p. 1059-69.
26. Watts, D.J. and S.H. Strogatz, *Collective dynamics of 'small-world' networks.* Nature, 1998. **393**(6684): p. 440-2.
27. Liu, J., et al., *Systems-level analysis of risk genes reveals the modular nature of schizophrenia.* Schizophr Res, 2018. **201**: p. 261-269.
28. Shim, M., et al., *Disruptions in small-world cortical functional connectivity network during an auditory oddball paradigm task in patients with schizophrenia.* Schizophr Res, 2014. **156**(2-3): p. 197-203.
29. Rakic, P., *Evolution of the neocortex: a perspective from developmental biology.* Nat Rev Neurosci, 2009. **10**(10): p. 724-35.
30. Lyall, A.E., et al., *Dynamic Development of Regional Cortical Thickness and Surface Area in Early Childhood.* Cereb Cortex, 2015. **25**(8): p. 2204-12.
31. Tau, G.Z. and B.S. Peterson, *Normal development of brain circuits.* Neuropsychopharmacology, 2010. **35**(1): p. 147-68.
32. Deoni, S.C., et al., *Mapping infant brain myelination with magnetic resonance imaging.* J Neurosci, 2011. **31**(2): p. 784-91.
33. Richman, D.P., R.M. Stewart, and V.S. Caviness, Jr., *Cerebral microgyria in a 27-week fetus: an architectonic and topographic analysis.* J Neuropathol Exp Neurol, 1974. **33**(3): p. 374-84.
34. Kroenke, C.D. and P.V. Bayly, *How Forces Fold the Cerebral Cortex.* J Neurosci, 2018. **38**(4): p. 767-775.
35. Hilgetag, C.C. and H. Barbas, *Developmental mechanics of the primate cerebral cortex.* Anat Embryol (Berl), 2005. **210**(5-6): p. 411-7.
36. Van Essen, D.C., *A tension-based theory of morphogenesis and compact wiring in the central nervous system.* Nature, 1997. **385**(6614): p. 313-8.
37. Price, D.J., *Lipids make smooth brains gyrate.* Trends Neurosci, 2004. **27**(7): p. 362-4.
38. Kingsbury, M.A., et al., *Non-proliferative effects of lysophosphatidic acid enhance cortical growth and folding.* Nat Neurosci, 2003. **6**(12): p. 1292-9.
39. Narr, K.L., et al., *Mapping Cortical Thickness and Gray Matter Concentration in First Episode Schizophrenia.* Cereb Cortex, 2005. **15**(6): p. 708-719.
40. Schultz, C.C., et al., *Reduced cortical thickness in first episode schizophrenia.* Schizophr Res, 2010. **116**(2-3): p. 204-9.
41. Bois, C., et al., *Cortical Surface Area Differentiates Familial High Risk Individuals Who Go on to Develop Schizophrenia.* Biol Psychiatry, 2015. **78**(6): p. 413-20.
42. Homan, P., et al., *Structural similarity networks predict clinical outcome in early-phase psychosis.* Neuropsychopharmacology, 2019.
43. Liu, Z., et al., *Resolving heterogeneity in schizophrenia through a novel systems approach to brain structure: individualized structural covariance network analysis.* Mol Psychiatry, 2021.